ON THE PRACTICALITY OF A FAMILY OF POP-UP PARABOLIC REFLECTORS

G. Greschik*
Department of Aerospace Engineering Sciences and
Center for Space Construction
University of Colorado, Boulder, CO 80309-0529

Abstract

The transformation of doubly curved surfaces, without affecting their geometric integrity, into quasi-foldable mechanisms via surface discontinuities is a recently proposed approach to self-deploying ("pop-up") reflectors. The marriage of surface accuracy and kinematic simplicity this concept represents may be especially attractive for small satellite antenna applications, once certain questions of practicality are answered. This paper is to summarize these questions and to quantitatively examine one of them — stowage efficiency — in the context of parabolic reflectors. First, a structural classification of deployable antenna dishes is put forth and the concerned pop-up concept is introduced. Some of the mechanical and geometric characteristics of the latter are briefly reviewed next, and the family of deployable reflectors it represents is illustrated via breadboard demonstration models. A brief study follows, wherein the stowage efficiency of the most promising proposed configuration is shown to be competitive with existing technology. This comparison is enabled by the *stowage ratio* ϑ, defined herein as a general measure of stowage efficiency independent of reflector structure and size. Finally, conclusions are drawn and functional, manufacturing, as well as further research issues are summarized.

Nomenclature

r	distance from paraboloid axis
z	height above vertex along paraboloid axis
$p = F$	paraboloid parameter = focal length
D	deployed dish diameter
d, h	cylinder diameter, height
V	volume
ρ	radius of shell bending
R, R_i	sphere radius; shell radius of curvature in dir. i
$\kappa_i = 1/R_i$	shell curvature in direction i
A, B, C, D	incision patterns/configuration types
$()_E$	reference to configuration type E
ϑ	stowage ratio

1. Introduction

The unfoldability of doubly curved surfaces in the traditional sense of the word is at the heart of the challenge of (parabolic, spherical, etc.) reflector dish deployment. No ideal answer to this challenge exist: the multitude of deployment concepts which have been proposed during the past decades all incrementally further the frontiers of existing technology via ever newer compromises between conflicting goals. None of the variety of involved ideas represents a breakthrough, and no breakthrough appears to be imminent either.

The deployment concept investigated in this paper — the application of discontinuities ("incisions") to flexible shell surfaces to transform them into quasi-foldable mechanisms — contributes to the wealth of dish deployment methods in two distinct means. First, via its novelty and the variety of possible means of its application, it represents a new family of deployable structures (not just reflector dishes). Second, it is characterized by a unique combination of advantages which may prove optimal for some missions. These advantages include (a) kinematic simplicity, (b) the theoretically perfect accuracy of the deployed surface, and (c) considerable freedom of deployment mechanism design, including the ease of providing stowed state symmetry for deployable dishes. Among its disadvantages, (a) the potential sensitivity of the surface accuracy to environmental effects and (b) a less than ideally compact stowed state for certain configurations are the most significant. Beyond the concept's qualitative analysis, the goal of the present paper is to quantitatively assess its stowage efficiency for some of its fundamental applications to no-offset parabolic dishes and also to highlight some further operational and manufacturing issues of practicality.

To this end, deployable antennas are reviewed

* Research Associate, Member AIAA.

first. In particular, a structural classification for them is offered to establish a framework for the discussion of the considered pop-up deployment concept to follow. The family of deployable parabolic dishes associated with the deployment concept is illustrated next for a few example configurations, the kinematic feasibility of which is shown via breadboard demonstration models. Subsequently, the stowage efficiency of the most promising demonstrated version is assessed for a realistic scenario and shown to be competitive with other dish deployment approaches. This comparison is enabled by the *stowage ratio*, a herein proposed general measure of deployable reflector stowage efficiency, applicable independent of reflector size and structure.

Finally, some functional, manufacturing, and design concerns which are the subject of ongoing research are summarized.

2. A review of deployable antenna concepts

Research interest in the space age-old challenge of antenna dish deployment was at its height during the 1980's — an era marked by NASA conferences on large space systems and space antenna systems technology[1, 2, 3] as well as by an array of national and international research efforts[38]. Work on the mechanical aspects of antenna technology has since withdrawn from the limelight of general professional interest. This is due both to the lack of a breakthrough and the recent dramatic progress of electronic antenna technology (phased array antennas, signal processing and filtering techniques, etc.). On the other hand, the lack of a breakthrough has also continued to motivate work within the field — an activity subdued in comparison with the past, yet, with a revived importance due to the current emphasis on small and cheap spacecraft against the backdrop of ever-increasing communication needs (larger antenna apertures, multi-band communication, etc.).

The decades of research on reflector dish deployment has produced a wealth of concepts and ideas. The abundance of these propositions is perplexing — one who sets out to review them or to place a new innovation into the framework of previous achievements is compelled to construct a classification in order to create a meaningful perspective. This is attempted below from a structural viewpoint.

Considering how its surface shape is maintained when deployed, a deployable reflector dish can be considered either as a segmented, a stretched, a membrane, or a shell structure.

The surface of a segmented antenna[25,31] consists of a number of quasi-rigid tessellations, each with a surface accuracy compromised by manufacturing tolerances only[29]. The high stiffness of the individual segments enables them to maintain their intended shapes, while a backup structure ensures the overall accuracy of the reflector surface assemblage. The primary advantages of this concept — surface continuity, high accuracy, and stiffness — are highly desirable for applications such as advanced communication antennae, submillimeter astronomical observatories, and microwave radiometers[4,23].

However, the source of the concept's advantages, viz., the rigidity of the solid antenna segments, is also the cause of its major disadvantage: a conflict between packaging efficiency and ease of deployment. This results that segmented reflector deployment either involves rather complex mechanisms[31, 41, 24, 6], a less then optimal compactness of the stowed state[42], or expensive extravehicular activity[30].

An antenna belongs to the second class (stretched reflectors) if its reflecting surface is stretched to shape via discrete structural components. The surface is either a wire mesh (mesh antennae[32, 9]) or a continuous membrane[45,44], and it is an approximation of the ideal shape typically with planar facets[36,28,43] or with cylindrical gores[15,44]. The members which stretch the surface to shape may involve (a) a truss[12,10,43], (b) booms[33,9], (c) a cable or a cable-and-catenary system[33,28,43], and/or (d) radial ribs with[27] or without[15,44] circumferential stiffener (and surface support) rings.

The major advantage of stretched reflectors over segmented ones is the light weight and flexibility of their reflecting surfaces, which permits very efficienct stowage and which allows the application of a variety of simple[45] and complex[28,33]innovative deployment (and surface support) systems to accommodate varying deployment and functional requirements.

The price of design flexibility, however, is the actual mechanical flexibility of the reflecting surface, which allows the improvement of operational accuracy — limited by geometric surface approximations and by shape sensitivity to environmental effects — only at the cost of increased support structure complexity[36]. Thus stretched antennae are limited to medium-to-high accuracy applications with approx. 1 to $40\,cm$[38]wavelengths (land mobile communications, direct broadcasting, Earth surface characteristic and atmospheric monitoring, deep space probes, etc.). The application of mesh reflectors to smaller wavelengths is also limited by the discontinuities of the mesh surface.

Membrane antennae (the third structural class considered), are similar to stretched ones in that it is tension which makes their reflecting surfaces attain (and, oftentimes, maintain) their shape. For membranes, however, this tension is due *not* to stretching by *discrete* structural elements, but to forces distributed over the antenna surface. The latter are most often provided via pressurization by gas or by an elastic spongy substance (although examples for non-structural support also exist[13]). In the former case (inflatable antennae[14, 37]), the shape of the inflated membrane is typically stabilized not by pressure itself but by rigidization — i.e., by imparting to it an appropriate stiffness once deployed. Two common approaches to this are (a) to impregnate (some of) the membrane laminae with a matrix which hardens in space[35], and (b) to apply an initial relatively high pressure to yield (one or more) soft metal (aluminum) layers incorporated into the membrane[16]. (No such rigidization is typical when pressurization — or "negative pressurization" — is via a spongy substance[39].) The reflecting surface is typically approximated via an assemblage of cylindrical gores[14, 37].

The membrane concept eliminates the often cumbersome deployment mechanisms and surface support systems of stretched antennae while it allows very compact packaging. For most current materials, however, the inextensibility of the membrane necessary for the required shape accuracy is too difficult to realize without a bending stiffness which, in turn, may result in the rupturing or wrinkling of the material when stowed.

Further, the shape of large membranes is sensitive to environmental effects — a problem which can be alleviated only with increased structural complexity, e.g., with internal cable elements[35] or with the application of the inflatable concept to reflector segments, rather than to the reflector as a whole[34]. (Although one non-structural means of distributed membrane support, viz., electrostatic shape control, has been shown to effectively solve the inaccuracy problem[18], the need for a backup structure to support the control devices necessary for this eliminates the packaging and deployment advantages of more conventional membrane antennas.)

These problems, as well as the lack of in-space experience with this class of reflectors, render current membrane antenna technology experimental.

The last category, shell reflectors, can be seen as a transition between the segmented and membrane ones, in that they also have a continuous reflecting surface but one which possesses a finite bending stiffness — as opposed to the, ideally, zero and infinite bending stiffnesses which characterize the other two classes. Their reflecting surface is thus a true elastic shell — the mechanical characteristics of which are utilized for shape stabilization.

The accuracy of shell reflectors' surfaces is thus limited by manufacturing tolerances only, and their deployment may be powered by the shell's elastic strain energy when stowed ("pop-up" deployment). The price for this combination of simplicity and accuracy is (a) an often less than ideally compact stowed state — which is due to the finite stiffness of the surface — and (b) the need for some additional (such as edge-) support in the deployed state, without which the shell could easily undergo bending distorsions. Two reflectors of this class are the one-piece dish of Composite Optics, Inc.,[40] and the LDA furlable strip reflector[39]. When stowed, the one-piece reflector is rolled into a cigar-shaped bundle, while the furlable strip concept involves several rolls for strips across the reflector surface. The one-piece concept involves a retracted state (a) without a rotational symmetry about the dish axis and (b) of extreme aspect ratios, while the surface subdivision of the furlable strip approach demands extensive support in the deployed state. (The recently proposed[19, 20] family of shell reflectors, made "foldable" via surface discontinuities, is discussed in the body of this paper.)

Hybrid structures which involve more than one of the above four concepts also exist[5].

This paper focuses on the practicality of a novel type of one-piece shell reflector — a smooth self-deployable shell without joints — which, unlike the Composite Optics one-piece reflector[40], has a stowed state of a (close to) rotational symmetry about the dish axis. This is achieved via quasi-folding the reflector's constituent shell, a process enabled by lines of discontinuity (referred to herein as "incisions") which define distinct but interconnected surface parts to form a foldable mechanism. The incisions, not affecting the overall geometric integrity and shape of the reflector and not interrupting surface continuity on the wavelength scale, do not corrupt accuracy and radiometric characteristics. Moreover, their adverse effects on reflector dynamics is also limited because the continuous surface parts they define have considerable stiffness on their own due to their doubly curved geometry and, further, they comprise an integrated system. The map of the incisions can be varied according to the folding mechanism and reflector characteristics desired. A detailed description of this concept and some of its practical issues follows.

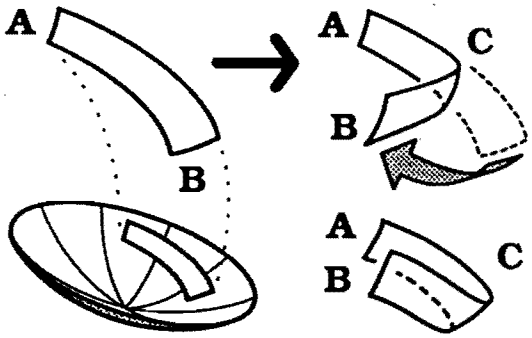

Figure 1: Folding a doubly curved shell strip.

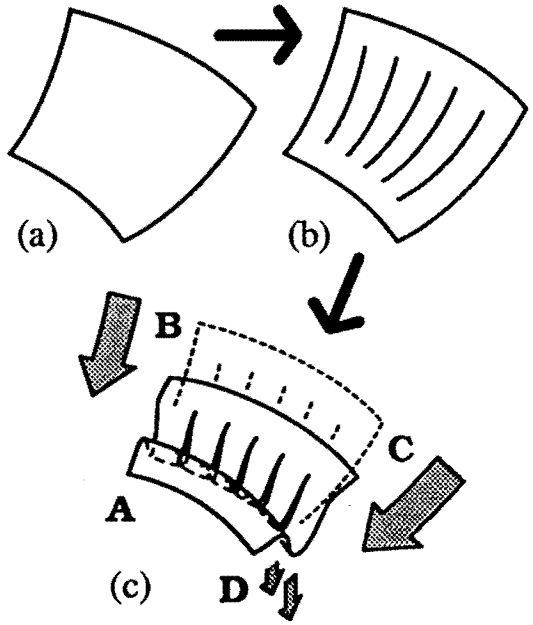

Figure 2: Folding a rectangular surface patch.

3. Forming a deployment mechanism via incisions

This section describes the a novel concept of "pop-up" reflectors — the use of incisions to transform doubly curved surfaces, without affecting their geometric integrity or shape, into quasi-foldable mechanisms.

3.1 Folding a doubly curved strip

A doubly curved surface (one with a non-zero Gaussian curvature) can not undergo folding in the traditional sense of the word, because its fold lines need be curved and, consequently, no finite surface segment could pivot about them without extensional deformations. If, however, the notion of a fold is considered not in the restrictive sense of a crease line but as a zone of intense bending (cf. the "folding" of a carpenter tape), folding and doubly curved surface geometry are no longer incompatible.

This is illustrated in Fig. 1 for a strip cut out of a paraboloid. Note that the simplicity of the parabolic surface in this example is not significant: one can fold a doubly curved strip even in the degenerate case of a curved tubular geometry, as demonstrated via the roll-up — the forming of a fold of indefinite length — of a helically shaped tubular strip[21, 22]. Apparently, any strip cut out of a sufficiently smooth shell is foldable, and, if the latter is thin enough, the folding is elastic. (However, closed form expressions for the stiffness and geometric properties of general folds — unlike those for a uniform, cylindrical strip[8] — can not be found in most cases.)

Despite the applicability of carpenter tape folding to doubly curved shell strips, however, past applications of the elastic bending of shells into elbows to effectively produce self-deployable folds mostly involve developable surfaces (cf. carpenter tape "hinges" or stiffeners[44,12] for straight and uniform sections or foldable tubular members[17]). The "carpenter tape" rib stiffeners of the intended final version of the CRTS reflector[44], which will have a doubly curved surface geometry in the final realization of the concept since they are to follow parabolic contours, are an exception, rather than the rule.

3.2 A foldable surface cell

The foldability of virtually any doubly curved strip and the fact that a doubly curved surface can always be subdivided into strips suggest that, at the cost of a surface subdivision, any general surface might be rendered foldable. This is apparently so for a rectangular surface patch, as illustrated in Fig. 2.

To fold the patch (Fig. 2 (a)), a number of slits aligned with one of the two "parallel" edge pairs of its (curved) rectangle are applied to its surface such that the strips thus produced are left interconnected at their ends (Fig. 2 (b)). This produces a set of similar strips arranged next to one another so that each of their two ends is attached to one of a pair of "transverse" strips (**AD** and **BC**) which serve as closures of the set. This assemblage can be folded, as illustrated in Fig. 2 (c), via moving the **AD** and **BC** transverse strips towards one another while concurrently folding the parallel ones (grey arrows).

Note that Fig. 2 (c) is misleading in suggesting a smooth folding process. In reality, the folds would form amidst local stability phenomena (warping and "popping") which would make the development of the fold mechanism non-smooth. Although this may be of concern for some applications, it does not affect the overall kinematic feasibility of the mechanism. Accordingly, it is paid no further attention herein.

The foldability of a mechanism produced via incisions (e.g., Fig. 2) is due to the individual strip folds, which function as *de facto* hinges with (constrained) bending, torsional, and translational degrees of freedom. That how much flexibility is imparted by the folds to a particular shell being folded depends on the geometry of the latter. If the surface to begin with is flat enough to allow carpenter tape folding even without incisions, then the latter are not essential to folding — they only increase the flexibility of the shell and its folding mechanism. Apparently, however, if the continuous geometry does not permit the development of a particular desired folding mechanism without stretching, the incisions make a qualitative difference.

(Accordingly, the incisions that enable folding can also be interpreted as a means to relieve the stretching (membrane stresses) which would develop if folding of the continuous shell were attempted. In this context, the concept herein concerned is related to the application of incisions to foldable tubes to relieve stress states which would otherwise impede deployment[26].)

Note that if the surface patch, as suggested in Fig. 2, has a positive Gaussian curvature (it is elliptic, or "dish-like"), the parallel strips are uniformly oriented and, consequently, they will generally tend to buckle and fold uniformly.

Having identified the pattern in Fig. 2 as a foldable mechanism, one is tempted to, in the spirit of Escher and Fuller, repetitively apply it as a cell of symmetry to particular surfaces in order to render them foldable. As described in the next section, however, the "verbatim" application of this approach to parabolic dishes is not desirable. Nevertheless, this case is discussed herein as a reference scenario for the discussion of practical derivative configurations to follow.

4. Repetitive application to a dish

A straightforward application of the rectangular incision pattern of Fig. 2 to a dish, referred to herein as the *simple straight pattern*, is illustrated in Fig. 3. The patch pattern is mapped with the incisions circumferentially aligned onto identical "pie"-shaped

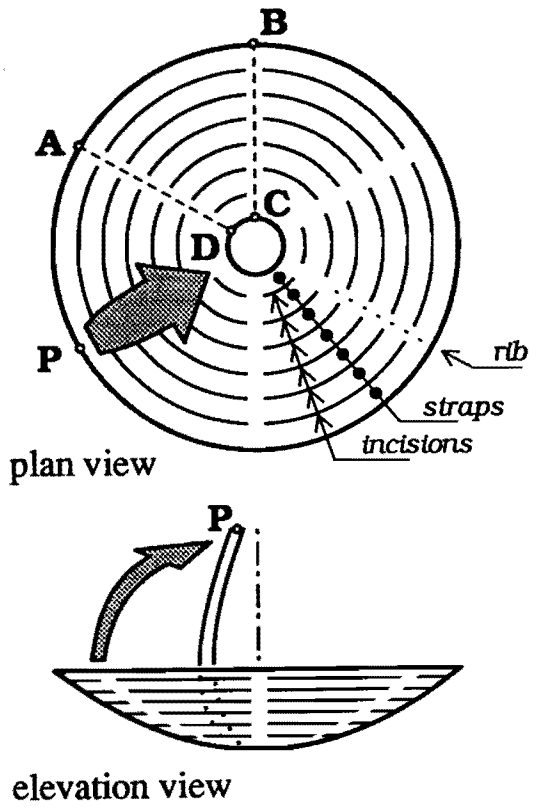

Figure 3: Simple straight pattern.

constitutive dish segments. Accordingly, two kinds of strip are produced: circumferential ones between the parallel incisions (internal to each dish segment) and radial ones to which the ends of the former are attached (shared by adjacent segments). These are referred to as *straps* and *ribs*, respectively (Fig. 3).

The pattern suggests that if the ribs are folded (and bent) upwards and towards the dish axis (as shown for an individual rib in the lower part of the figure), the distances between the end points of all straps decrease and the straps fold: a multiple version of the mechanism of Fig. 2 (c) results. Therefore, concurrently folding all ribs inward should result a stowed state akin to a closed umbrella, in which the folded straps correspond to the umbrella's fabric. (As alluded to previously, the dish-like surface shape predestines a uniform outward folding of the straps when driven by compression across the foldable cells — the closing of the ribs.)

A simple means to control deployment (and folding) would be through the rib ends — e.g., via cables in between, or between them and point(s) along the dish axis. Such control, however, can not enforce the umbrella-like kinematics due to the high stiffness of the straps close to the dish center with respect to

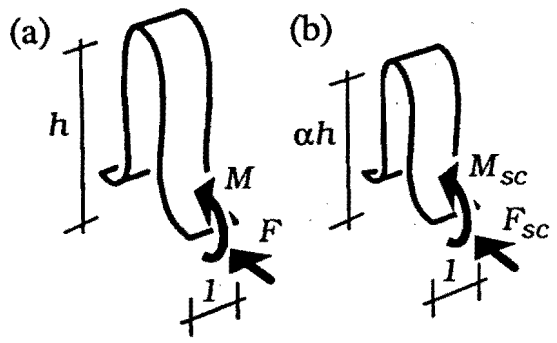

Figure 4: The scaling of a strip's longitudinal geometry with factor α.

those at a distance: a difference so great that, if the rib ends are pulled together, the central part of the dish remains virtually undeformed and only its edge folds inward. Some reasons of this phenomenon are reviewed in Section 4.1.

Another problem of the pattern of Fig. 3 is stress concentrations — a concern of particular relevance to composite shells — is discussed in Section 4.2.

4.1 The stiffness of the dish center

The forces and moments needed to fold (and to maintain the folded state of) the straps of the simple straight patters — the end responses of the folded straps — need to be much higher at the center of a parabolic dish than away. There are a few easily identifiable factors that contribute to this, some of which have been investigated (without accounting for their interaction) in[20, 19].

As shown therein, a scaling of the longitudinal geometry of a strip with a factor α while preserving its cross section geometry (Fig. 4 (a) to (b)) scales the moment and force responses with factors of α^{-1} and α^{-2}, respectively:

$$M_{sc} = K_M \kappa_{sc} = \alpha^{-1} K \kappa = \alpha^{-1} M \qquad (1)$$

and

$$F_{sc} = \frac{dM_{sc}}{dl_{sc}} = \frac{d[\alpha^{-1}M]}{d[\alpha l]} = \alpha^{-2}\frac{dM}{dl} = \alpha^{-2}F \qquad (2)$$

where K denotes the strip cross section stiffness for bending (or torsion) and κ is bending curvature (or torsion). (The force responses include both shear and axial forces, the latter herein being direct derivatives of the former.) This highlights a trend of inverse proportionality with the strap length and its square of the moments and forces to be exerted onto the strap ends.

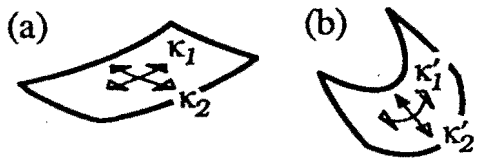

Figure 5: The bending of a doubly curved patch.

The strap lengths' order-of-magnitude variation for the umbrella pattern thus develops differences of one and two orders of magnitude in the end responses for torsion/bending and forces. Obviously, highly flexible ribs of close to uniform shapes can not provide, without reinforcement, such a wide a range of support intensity for the straps while smoothly bent as desired for the umbrella-like stowed shape. For this, either a softening of the straps (say, via a thinner shell) at the dish center or a stiffening of the ribs is needed. (The feasibility of the latter has been confirmed via a model with stiffeners attached to the outside of the ribs.)

Note that the rib loads the strap end *bending* moments represent are lessened by the dish symmetry (cf. Fig. 3): the strap moments on the opposite sides of the ribs tend to cancel out as the number of dish segments increases. However, for a particular dish with a particular order of symmetry, this bending increases towards the dish center with the increase of the therein maximal paraboloid surface Gaussian curvature. This can be seen (cf. [20, 19]) from considering the bending of a doubly curved surface patch of Gaussian curvature G and strain-free principal curvatures κ_1 and κ_2 (where the relative magnitudes of κ_1 and κ_2 are insignificant), as shown in Fig. 5. The stretch-free bending of the strip along principal direction 1 into (co-linear) principal curvatures κ'_1 and κ'_2 (which means no torsion in the $1-2$ reference frame) implies

$$\kappa_1 \kappa_2 = \kappa'_1 \kappa'_2 = G \qquad (3)$$

Assuming that the shell is sufficiently thin, the vector $\underline{\mathbf{m}}$ of shell bending moments m_1 and m_2 can be calculated via the appropriate part of $\underline{\underline{\mathbf{D}}}$, the plate flexural stiffness matrix[7] and using (3) as

$$\underline{\mathbf{m}} = \begin{pmatrix} m_1 \\ m_2 \end{pmatrix} = \underline{\underline{\mathbf{D}}} * \Delta\underline{\kappa} = D(\kappa'_1 - \kappa_1) \begin{bmatrix} 1 & \nu \\ \nu & 1 \end{bmatrix} * \begin{pmatrix} 1 \\ G/(\kappa'_1 \kappa_1) \end{pmatrix} \qquad (4)$$

in which $D = Et^3/(12(1-\nu^2))$ is the plate flexural rigidity with E, ν, and t the Hook's modulus, the Poisson's ratio, and the shell (plate) thickness, respectively, and "$*$" symbolizes the inner product.

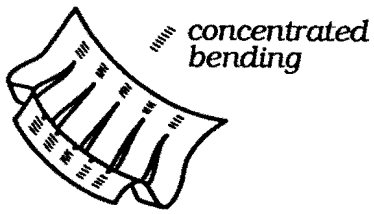

Figure 6: The concentration of bending deformations for a folded and concurrently bent patch.

The doubly curved geometry of the strip is reflected in (4) by the second component of the $\Delta\underline{\kappa}$ vector. For a given Gaussian curvature G, the sign of $(\kappa_1'\kappa_1)$ determines whether the geometry implies an increase or a decrease of m_1 for the $\Delta\kappa_1 = (\kappa_1' - \kappa_1)$ curvature change — whether the geometry stiffens or softens the shell against bending in the 1 direction. For a paraboloid, where $G > 0$, opposite signs of κ_1' and κ_1 stiffen the fold — the case for the surface straps considered (Fig. 3). This stiffening effect is increased by the increasing Gaussian curvature

$$G = \kappa_{cir}\kappa_{rad} = \frac{\kappa_{cir}^2\, 4p^2}{4p^2 + r^2} = \frac{4p^2}{(4p^2 + r^2)^2} \qquad (5)$$

toward the center of the paraboloid

$$z = r^2/(4p) = (x^2 + y^2)/4p \qquad (6)$$

Although the interaction of torsion, bending, as well as shear and axial forces in the context of a bent real strap-and-rib assemblage are more complex than the above arguments reflect, this simplistic derivation, nevertheless, suffices in highlighting some trends to provide a partial analytical explanation for the experimentally observed high dish center stiffness associated with the simple straight incision pattern.

4.2 Stress concentrations

The lines of surface discontinuities effect stress concentrations in the folded state via two distinct mechanisms. First, their endpoints (*de facto* 360° corners) engender high stresses under almost any straining — a problem related to such discontinuities in any structure. Second, the concurrent rib and strap bending, characteristic to the desired folding mechanism of Fig. 3, results in concentrated rib bending at the lines (or thin bands) between adjacent straps (Fig. 6) since the lack of space between subsequent ribs' connections to the latter prohibit gradual bending.

Stress concentration at the incision ends may be lessened via "classic" techniques, such as round holes,

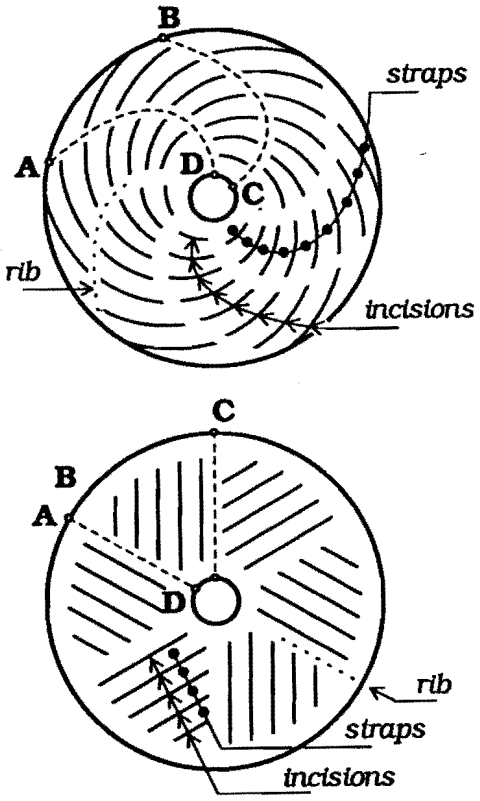

Figure 7: Non-practicable direct applications of the rectangular foldable patch pattern.

as exemplified in Section 5. The bending concentrations, on the other hand, can be removed by providing, via auxiliary incisions, sufficient rib lengths ("weak zones") for the development of smooth bending. This, however, leads to a rather complicated refinement of the incision pattern in the context of the simple straight pattern (cf. [20, 19]). Nevertheless, auxiliary incisions which define weak zones for controlled bending and thus control the overall folding pattern remain an important design tool for the practical configurations discussed in Section 5.

4.3 Other configurations via direct repetition

Other direct applications of the patch pattern of Fig. 2 to dishes, illustrated in Fig. 7, are not practicable either. Their stowed states, which appear to have the promise of higher compactness that of the umbrella shape due to their twirled geometries, can not be realized offset due to a number of kinematic difficulties. This turns one's attention towards derivative configurations where the incision map is specifically

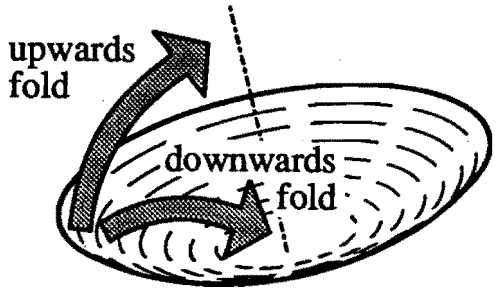

Figure 8: The upward and downward folding of the dish edge.

	dish center	
	soft	hard
continuous edge folded...		
...upwards	A	–
...downwards	–	B
discontinuous edge folded...		
...upwards	C	–
...downwards	–	D

Table 1: The classification of considered configurations $A - D$.

tailored to produce certain deployment mechanisms.

5. Practicable configurations

Two dominant characteristics of parabolic dishes with surface discontinuities are (a) the stiffness of the dish center (cf. Section 4.1) and (b) the expanse of the dish skirt — one mechanical and one geometrical challenge to foldability and to stowed state compactness, respectively. A convenient way to classify workable dish incision configurations is through how these challenges are met.

The distinction between a *hard* and a *soft* centered dish is herein made depending on whether a (non-negligible) central part of the dish is left continuous or it is weakened via incisions. On the other hand, if the dish rim forms a continuous ring (such as in Fig. 3), the edge is termed *continuous*, while if it is subdivided by incisions, it is referred to as *discontinuous*. Further, the dish perimeter can either be folded (pulled) *upwards*, away from the bottom of the dish (Fig. 3), or *downwards*, into the dish (see Fig. 8).

The possible combinations of these options are shown in Table 1, with A through D referring to the cases chosen for further study. The two combinations of features not investigated further are (a) the softening of the dish center and the concurrent folding of the dish perimeter into the dish cup ("downward folding") and (b) leaving a considerable zone around the dish center intact but folding the dish perimeter upwards, rather than downwards. The former case is deemed spurious, while the latter would yield a stowed state compactness to be easily improved by lessening the size of the rigid dish center — by making the dish soft-centered.

The classification of Table 1 is not exhaustive — configurations outside the listed categories also exist.

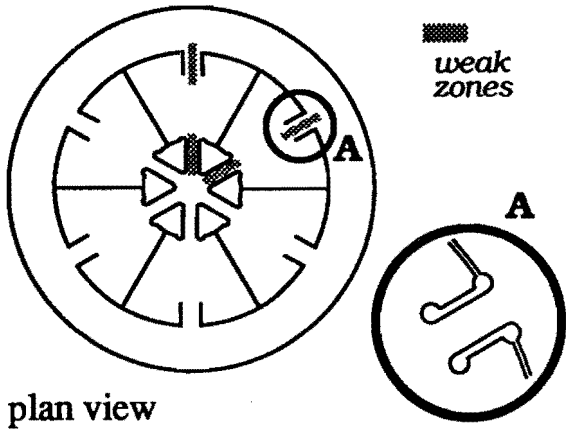

Figure 9: Incision pattern: soft dish center with upward-folded continuous rim.

5.1 Example configurations

Configurations A through D (Table 1) are illustrated via plastic demonstration models with an approximate deployed dish diameter $D = 18.2\,cm$ and focal length $p = 4.75\,cm$ — a low F/D ratio of 0.26.

5.1.1 Configuration class A. Considering the reasons behind the stiffness of the dish center for the simple straight pattern discussed in Section 4.1, it is apparent that the center can be softened only by incisions radially aligned (so that the strap lengths not be limited by the proximity of the paraboloid vertex). This is so in the design of Fig. 9, with the continuous dish rim folded upward. (The rim can be perceived as to echo the overall circumferential character of the simple straight pattern — Fig. 3.)

A (partially) folded state of this design is shown in Fig 10. The pie-shaped surface patches defined by the radial incisions fold under and top of one another

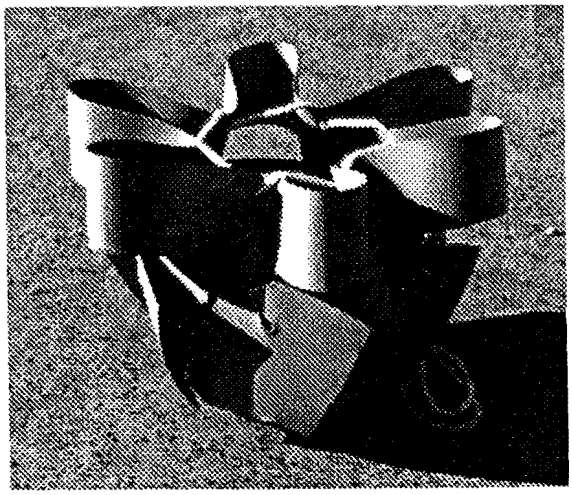

Figure 10: A partially folded state for the pattern of Fig. 9.

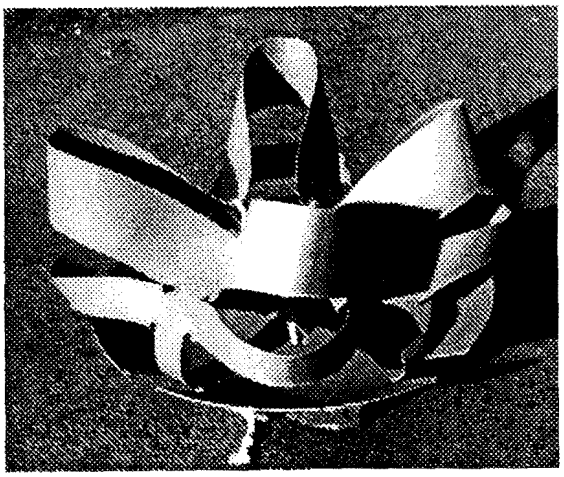

Figure 12: A partially folded state corresponding to the pattern of Fig. 11.

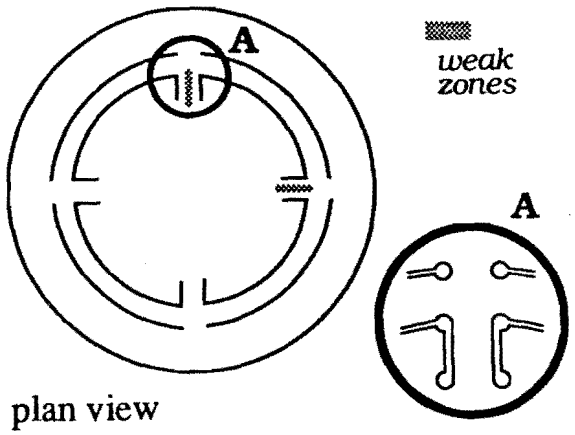

Figure 11: Incision pattern: hard dish center with downward-folded continuous rim.

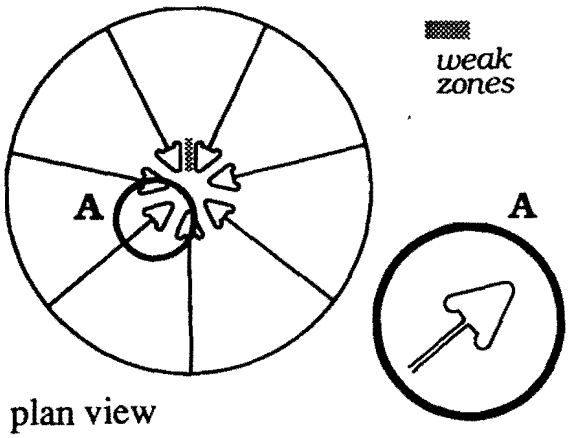

Figure 13: Incision pattern: soft dish center with upward-folded discontinuous rim.

in a manner similar to the "petals" of the Dornier segmented deployable antenna[25]. They, however, are integrated in a unified system not by hinges at their inner ends but by elastic folded shell strips at both the inner and outer ends. The application of the radial incisions to soften the dish center is, apparently, successful: the stowed state is of the shape of a tall, slim basket.

5.1.2 Configuration class *B*. One way a continuous dish perimeter can be downward-folded into a rigid dish center is according to the pattern of Fig. 11. A photograph of the (partially) stowed state of a model accordingly built is shown in Fig. 12. Although the overall circumferential character of the involved incisions can clearly be seen as derivatives of the simple straight pattern (Fig. 3), auxiliary radial incisions are also involved. The latter are to define sufficient rib lengths for the development of rib folds without undue stress concentrations (cf. Section 4.2).

5.1.3 Configuration class *C*. Stowage compactness can be greatly increased at the cost of sacrificing the continuity of the dish perimeter. For a dish center softened via radially aligned incisions and an upward-folded stowed scenario, for which a case of continuous dish rim was demonstrated in Section 5.1.1, a design with discontinuous rim is exemplified in Fig. 13. (The number of segments has been chosen as seven to make the design akin to that of Section 5.1.4, where, as

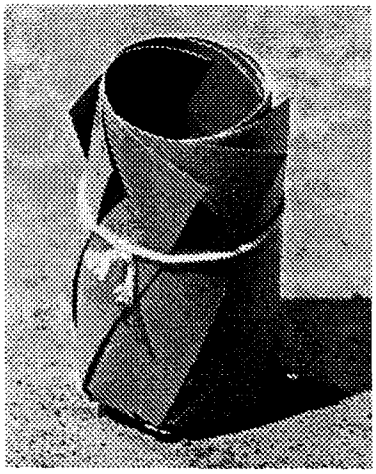

Figure 14: A partially folded state corresponding to the pattern of Fig. 13.

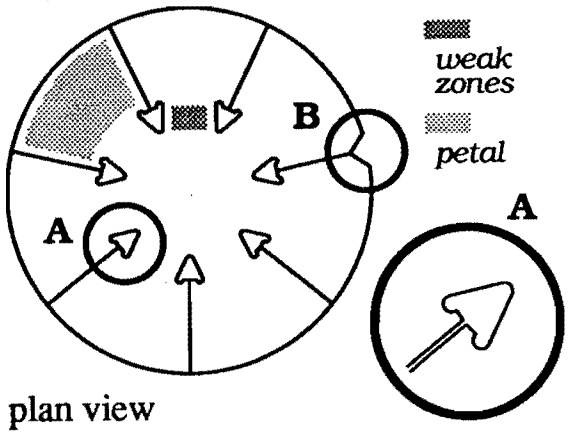

Figure 15: Incision pattern: hard dish center with downward-folded discontinuous rim.

therein discussed, this number is necessary.) A photograph of the stowed state of a model accordingly built is shown in Fig. 14. The circular symmetry of the stowed reflector petals is, again, that of the Dornier antenna[25] — viz., the sides of each petal are uniformly under and above the neighboring petals all the way around.

Note that the reflector petals are not only pulled together in the stowed state but are also bent into a cylindrical envelope (Fig. 14).

5.1.4 Configuration class *D*. Consider the fictitious process of gradually shortening the incisions of the previous example. As the stems of the petals thus move outward, a continuous dish center appears, with an expanse increasing at the cost of the petals' lengths. With (a) the relative length of the petals shortening and (b) their stems moving away from one another, their most compact stowed states of the Dornier antenna's circular symmetry will involve an increasing tilt, until they actually fold into the dish center, approximately when the petal lengths reach about one fourth of the dish diameter.

However, downward folding of the petals is possible much earlier — when the petal lengths still are only about one third of the dish diameter — if the stowed state symmetry is broken. One possible example of this, for the plan view in Fig. 15, is illustrated via its partially stowed state in Fig. 16. Note the lack of symmetry — one of the petals is under its neighbors on both sides, while another is on the very top of the stack. The overall kinematics of this configuration is reminiscent to the single ring precision segmented reflector *SCOPE*[31].

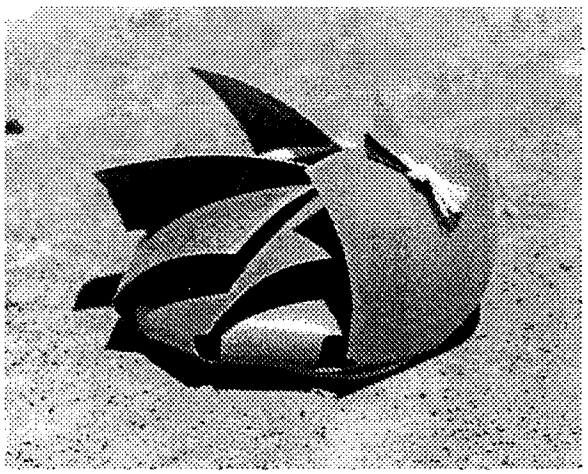

Figure 16: A partially folded state corresponding to the pattern of Fig. 15.

Properly shaping the outer petal edges or corners (detail **B** in Fig. 15) is a straightforward means to eliminate interference between the petal corners and the bent necks on the opposite side and thus to improve stowage compactness.

An important criterion for inward-foldability beyond those for petal size and shape is a limit of 60° on the angular widening of the petals. This limit, an obvious result of the circular geometry, translates into more than six dish segments — hence the choice of seven for the example.

5.2 Some design considerations

Despite crudity and a material choice inappropriate for real designs, the above models still reveal some

Model		A	B^*	C	D
Height	h_{model} $[cm]$	9.0	6.5	8.5	3.3
Diameter	d_{model} $[cm]$	9.0	13.0	3.5	8.5
...of cylindr. envelope					
Volume	V_{model} $[cm^3]$	570	860	82	190

* could be further compacted some by compressing the free loops of the dish perimeter into a smaller hull — cf. Fig. 12

Table 2: Approximate dimensions for cylindrical stowage envelopes for models $A - D$.

important features of the concerned configurations.

A trend of superior stowage efficiency for discontinuous rim designs (C, D) is boldly highlighted by the approximate stowage volumes, calculated from the dimensions of the cylindrical envelopes of the models' stowed states, listed in Table 2.

The lack of connection between the petals at their outer edge, however, significantly reduces the structural integrity of these dishes. This is most detrimental for model C, where the narrow petal stems are unable to sustain even an approximate paraboloid shape under gravity. Design D, the layout of which only quantitatively differs from that of C, is an attractive alternative: the wide petal stems more than balance the lack of edge support for stiffness — the qualitative investigation of the deployed model shows a stiffness comparable to the continuous edge designs A and B.

Beyond stiffness, however, design D also offers two further significant advantages. One, a healthy petal aspect ratio with structural and manufacturing advantages as well as a limited sensitivity to certain thermal effects. Two, the simplicity of the incision pattern and kinematics which allows hybrid shell/segmented dish designs where flexibility is limited to the petal necks and the petals are rigid. This may (a) simplify the design and manufacturing of the necks' laminate layout (not constrained by preferences and restrictions elsewhere), (b) offer (relatively) easy means of shape control via, e.g., smart structure concepts/piezoelectric laminates at the necks, (c) enable additional backup support with modest structural dimensions (extending to the inner petal edges only), and, finally, (d) facilitate the attachment of adjacent petal edges to one another after deployment.

Note that hybrid designs, and the above listed consequent advantages, could also be realized for configurations A and C. This, however, does not lessen the relative attractivity of design D, the simplicity and stiffness of which is superior to A and C regardless of the rigidization of the petals. Design B, which entails the least compact stowage, also involves the most narrow shell strips — the highest sensitivity to thermal gradient effects. Further, this design leaves little room for manufacturing parts other than the reflector center rigid.

An aspect of all demonstration designs which, although it does not correlate with desirability, still deserves a note, is how the stress concentrations (cf. Section 4.2) are alleviated via shaping the incision corners and edges. This is highlighted by insets **A** in Figs. 9 through 15. Note (a) the round holes at the incision ends and (b) that the weak necks (the loci of intense bending) are delimited by edges that join the circular holes at the incision corners ***tangentially***, at the extreme points of the latter. The latter ensures a smooth distribution of bending via a uniformly weak cross section along each neck's length — which would not be so if the circular hole at the neck's end locally narrowed it even further.

The stowage compactness of the most promising configuration, D, is assessed in the following for a realistic scenario.

6. Configuration D — stowage efficiency

To refine the crude relative assessment of stowage efficiencies in Table 2, realistic reflector geometry and material characteristics need to be considered. For compatibility with the relevant parts of reference[11], the antenna parameters therein chosen as representative to multi-purpose small satellite applications — a no-offset parabolic dish with $D = 120\,in = 3.048\,m$ diameter and an identical focal length F (i.e., $F/D = 1.0$) — are considered herein as well. The constitutive shell is a mid-surface symmetric 6-ply $P75/ERL1962$ laminate (of near-zero CTE) with 60° orientation offsets between adjacent plies and a $t = 0.254\,mm$ total thickness.

Since the variation (as a function of position within the dish) of shell curvatures in the radial and circumferential directions κ_{rad} and κ_{cir} for this geometry are relatively small (cf. (5), $F = p$), the dish shape is approximated as a sphere of average radius

$$\begin{aligned} R &= (R_{cir,ctr} + R_{rad,ctr} + R_{cir,edg} + R_{rad,edg})/4 \\ &\approx (6.10 + 6.10 + 6.28 + 6.68)/4 \\ &\approx 6.29\,m \end{aligned} \qquad (7)$$

in the following.

6.1 Strap and rib bending

What determines stowage compactness within the paradigm of most incision patterns (and the corre-

sponding deployment mechanisms) is how sharply — into how small a radius — the shell may be bent where needed. An accurate assessment of permissible strip bending radius, influenced by strip geometry, location, and orientation within the dish as well as by the laminate's orientation therein is beyond the scope of the present study. Instead, the results of reference [11] are considered, despite their approximate nature. The approximation involved is a result of software limitations[11] which prevented the analysis of the laminate's bending in the context of the doubly curved dish geometry. To still explore the limitations of shell bending, two scenarios have been analyzed in [11]: the bending of an initially (a) flat and (b) cylindrical laminate strip with the appr. $0.61\,m$ curvature of the latter oriented perpendicular to the direction of bending. This radius of curvature is one tenth of the smallest dish directional shell curvature radius (at the center — cf. (7) and (5)).

As shown in [11], both the initially flat and cross-curved cylindrical strips may bend into radii $\rho < 1.7\,in = 43.2\,mm$ with less then $19.5\,ksi$ maximum ply stress effected, if the ply orientation deviates less than $\pm 5°$ from an optimal direction. Consequently, and to conservatively account for the uncertainties of an extrapolation from these results to the actual doubly curved geometry, a general $\rho = 5\,cm$ is taken herein as the maximum permissible strip bending radius. A close to optimal ply orientation in the bent regions is assumed.

Note that, because [11] is concerned with deformations under pure bending only, the use of $\rho = 5\,cm$ as an approximate minimum radius of strip bending should be limited to cases when torsion, shear, and membrane effects are insignificant in comparison to bending. The stowed configuration D, studied subsequently, is seen as such.

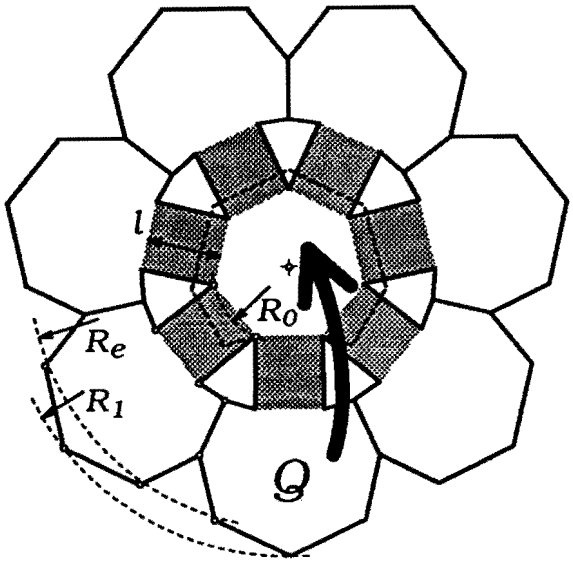

Figure 17: Example configuration of class D (hybrid design: flexible parts shaded).

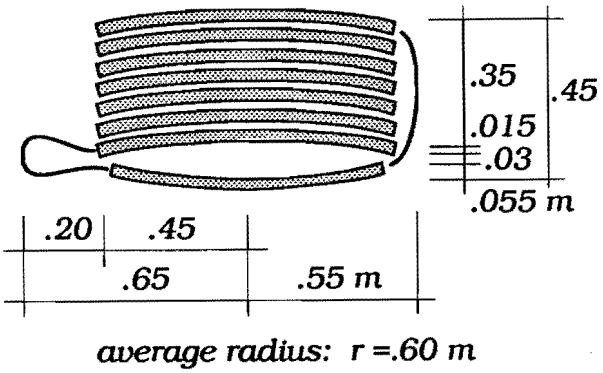

Figure 18: Schematic package cross section for the design of Fig. 17.

6.2 Stowage dimensions

One possible realization of configuration class D is illustrated in Fig. 17. The petals' outer edge is shaped to better fit the envelope delimited by the petal necks bent in the stowed state, as illustrated with a dashed line for petal Q. Consequently, the reflector's effective radius is less than the maximum radius: $R_e < R_1$. The petal necks' length is l.

A schematic cross section of the hybrid configuration's stowed state is shown in Fig. 18. The shown dimensions have been estimated as follows.

For the rigid panels (the dish center and the petals) thin laminate face-sheets with a honeycomb core of $1.5\,cm$ total thickness is taken, with $3.0\,cm$ deep stiffener ribs — yielding a total thickness of $4.5\,cm$. (The stiffener ribs' configuration left unspecified.) This thickness is padded with an $0.5\,cm$ margin to account for differences in geometry and orientation as well as the non-ideal alignment of subsequently stacked petals. This yields a stowage layer thickness of $5.0\,cm$ per petal — a total of $35\,cm$ for the stack of all seven petals. This considerable dimension necessitates long petal necks, estimated with a lower bound: $l > 0.40\,m$.

The cupping of the petal and of the dish center rigid panels is taken as an approximate $1.5\,cm$, from the spherical approximation (7) and expected maximum effective panel radius $0.40\,m$ (slightly less than the estimated maximum radius of $0.45\,m$ shown in Fig. 18). This adds to the bottom panel thickness (of

5 cm, see above) as well as to the 35 cm thickness of the stack of petals.

Due to the long necks (recall $l > 0.40\,m$), the minimum radius of bending estimated in Section 6.1 as $\rho = 5\,cm$ is not direcly relevant: the neck has sufficient length to allow for multiple bends and thus for a rather narrow gap between the dish bottom panel and the stack of petals. This gap is taken as $3\,cm$ — cf. Fig. 18.

From the minimum radius of shell bending estimated in Section 6.1 as $\rho = 5\,cm$ and the 40 cm minimum neck length, the lateral expanse of the folded necks beyond the perimeter of the panels is taken to be more than 10 cm but less than 20 cm. As the figure illustrates, this, along with the 45 cm maximum panel radius, results in an average cylindrical stowage space radius of 60 cm.

The estimated diameter and height of the cylindrical stowage envelope are, therefore, $d = 1.20\,m$ and $h = 0.45\,m$, yielding a volume of $V = 0.51\,m^3$.

6.3 Evaluation of efficiency

To enable the comparison of the stowage efficiency of dishes of different sizes and constructions, let the measure of stowage ratio ϑ be defined as the ratio of the stowage envelope's total surface to the area of the aperture plane covered by the reflector after deployment

$$\vartheta = \frac{stowed\ volume's\ surface}{covered\ area\ of\ aperture\ plane} \qquad (8)$$

As it involves the surface, rather than the volume of the stowed package, this measure is somewhat biased in favor of packages of balanced aspect ratios — a welcome bias for a single-number-based comparison.

Note that, as a dimensionless number, ϑ measures the pure "compactibility" of a given mechanism regardless of size — but, clearly, as a function of the *relative* measures of geometry (aspect ratios, etc.). Nevertheless, in a strict practical sense of the word, it can still not eliminate all scaling effects, since the latter do affect some relative dimensions within most structures.

Assuming cylindrical stowage envelopes, the stowage ratios for some segmented and hybrid-segmented dishes are shown in Table 3 (with the addition, for the sake of comparison, of the pure shell Composite Optics reflector). The herein concerned hybrid D variant of the newly proposed deployable dish is clearly competitive with existing technology.

Concept	D [m]	d [m]	h [m]	ϑ
SUNF	9.6	4.4	3.5	1.10
SUNF-2	15.0	4.4	6.6	0.69
COI**	3.0	0.5	3.0	0.72
GR-D**	3.0	1.2	.45	0.6 +
DORN	-	-	-	1.3*+
SCOPE	-	-	-	0.9*+

* estimated from figures without dimensions given
** without backup support
\+ one-digit precision signals lower accuracy

Table 3: Deployed diameters D, stowage cylindrical envelope diameters and a heights d and h, and stowage ratios ϑ for some deployable dishes (SUNF – Sunflower[42]; SUNF-2 – Sunflower descendant[25]; COI – Composite Optics, Inc.[11]; GR-D – Greschik, type D, hybrid example design; DORN – Dornier[25] without the feed; SCOPE – SCOPE[31]).

7. Summary

Variants of the application of a novel shell deployment concept — which involves surface discontinuities ("incisions") to make the surface quasi-foldable — to reflector dishes have been investigated, and the concept has been shown practical from the perspective of stowage compactness.

After a structural review of current deployable antenna technology, four fundamental configurations of the new deployment concept have been outlined, and their kinematic practicability has been demonstrated via breadboard demonstration models. Via a preliminary design study of the most attractive considered scenario, a stowage efficiency actually higher than those provided by a number of other current deployment approaches has been shown achievable. Instrumental to reaching this conclusion has been the herein defined dimensionless measure of *stowage ratio*, which relates the surface of the stowage volume to the surface of the reflector's aperture plane covered in the deployed state. This measure carries a welcome bias in favor of balanced aspect ratios of the stowed state, and it is directly sensitive to the relative dimensions within a concerned mechanism only. Due to the latter, its sensitivity to scaling effects is limited to the indirect impact of scaling to a structure's *relative* dimensions.

The practicality from the viewpoint of stowage ef-

ficiency demonstrated, a number of questions still remain to be answered before a future application of the incision concept. These, which are the subject of ongoing research, include:

1. the dynamic characteristics of the deployed surface and the sensitivity of surface accuracy to dynamic environments;
2. deployment control to optimize the dynamic effects of deployment on spacecraft;
3. optimal means of support in the stowed state and auxiliary support in the deployed state;
4. means to recover some of the structural integrity lost due to the incisions (e.g., the attachment of adjacent rigid petals to one another after deployment for hybrid designs);
5. effects of thermal loads;
6. active shape control;
7. manufacturing and design methodology;
8. the extent and effects of, as well as the optimal means to alleviate stress concentrations;
9. the use of piezoelectric laminates/smart structural concepts for some of the above.

Alternative incision patterns are also being sought.

8. Acknowledgements

The writer thanks Profs. Martin M. Mikulas and K.-C. Park for their inspiring cooperation, consultation, and he thanks Prof. K.-C. Park for his personal support. The support of the Center for Aerospace Structures and of the Center for Space Construction of the University of Colorado at Boulder during the course of this work is also gratefully acknowledged.

References

[1] Large Space Systems Technology (LSST) technical review. Conference Proceedings CP-2118, NASA, 1980. Second annual technical review held at NASA Langley Research Center, Hampton, Virginia, November 18-20.

[2] Large Space Antenna Systems Technology. Conference Proceedings CP-2269, NASA, NASA Langley research Center, Hampton, VA, December 30 – December 3 1982.

[3] Large Space Antenna Systems Technology. Conference Proceedings CP-2368, NASA, NASA Langley research Center, Hampton, VA, December 4–6 1984.

[4] Anon. The large deployable reflector (LDR) report of the Science Coordination Group. NASA JPL-86-46, NASA Jet Propulsion Laboratory, October 1986.

[5] J. S. Archer and W. B. Palmer. Antenna technology for QUASAT applications. In [3], pages 251–270.

[6] K. E. Ard. Design and technology study for extreme precision antenna structures. NASA Contractor Report CR-174861, NASA Lewis Research Center, Cleveland, OH, August 1985. Contract NAS3-23249. Harris Corporation, Government Aerospace Systems Division, Melbourne, FL.

[7] C. R. Calladine. *Theory of Shell Structures*. Cambridge University Press, Cambridge, GB, 1983.

[8] C. R. Calladine. The theory of thin shell structures 1888–1988. *Proceedings of the Institution of Mechanical Engineers*, 202(A3):141–150, 1988. Love Centernay Lecture.

[9] Harris Corporation. Development of the 15 m diameter hoop column antenna. NASA Contractor Report CR-4038, NASA, 1986. Final report. Contract NAS1-15763.

[10] J. V. Coyner. Box-truss development and its applications. In [3], pages 213–233.

[11] Principal Investigator Danley, E. D. Earth observing sensor development for geostat furlable microwave antenna reflector. SBIR 1st Phase Final Report NAS8-40114, NASA Marshall Space Flight Center, July 25 1994. Contract NAS8-40114. Composite Optics, Inc., San Diego, CA.

[12] J. A. Fager. Status of deployable geo-truss development. In [2], Part 1, pages 513–525.

[13] R. A. Freeland. Survey of deployable antenna concepts. In [2], pages 381–421.

[14] R. E. Freeland and G. Bilyeu. In-step inflatable antenna experiment. In *World Space Congress 1992, 43rd Congress of the International Astronautical Federation*, Washington, D.C., August 28 – September 5 1992. IAFn, 3-5, Rue Mario-Nikis, 75015 Paris, France. IAF-92-0301.

[15] R. E. Freeland, N. F. Garcia, and H. Iwamoto. Wrap-rib antenna technology development. In [3], pages 213–233. pages 139–166.

[16] G. J. Friese, G. D. Bilyeu, and M. Thomas. Initial '80s development of inflated antennas. NASA Contractor Report CR-182065, NASA Langley Research Center, January 1983. Contract NAS1-16663. L'Garde, Inc., Newport Beach, CA 92663.

[17] L. W. Gertsma, J. H. Dunn, and E. E. Kempke. Evaluation of one type of foldable tube. NASA Technical Memorandum TM X-1187, NASA Lewis Research Center, Cleveland, OH, December 1965.

[18] W. S. Gregorwich, H. A. Malliot, and A. K. Sinha. Large-diameter geostationary millimeter wavelength antenna concept. In R. L. Wright and T. G. Campbell, editors, *Earth Science Geostationary Platform Technology*, pages 69–82, Hampton, VA, 1989. Proceedings of workshop, September 21–22, 1988. NASA Conference Publication CP-3040.

[19] G. Greschik. The deployment of dishes with surface discontinuities. *Journal of Spacecraft and Rockets*, 1995. Submitted for publication.

[20] G. Greschik. The unfolding deployment of a shell parabolic reflector. In *The 36th AIAA/ASME/-ASCE/AHS/ASC a Structures, Structural Dynamics, and Materials Conference and AIAA/-ASME Adaptive Structures Forum*, Part 2, pages 1050–1059, New Orleans, LA, April 10–13 1995. AIAA-95-1378-CP.

[21] G. Greschik and K. C. Park. The deployment of curved closed tubes. In *The 36th AIAA/-ASME/ASCE/AHS/ASC Structures, Structural Dynamics, and Materials Conference and AIAA/ASME Adaptive Structures Forum*, Part 3, pages 1964–1975, New Orleans, LA, April 10–13 1995. AIAA-95-1395-CP.

[22] G. Greschik, K. C. Park, and M. Natori. Helically curved unfurlable structural elements: kinematic analysis and laboratory demonstration. *Journal of Mechanical Design*, 1995. Accepted for publication.

[23] NASA Task Group. Outlook for space. Technical Report NASA SP-386, January 1976.

[24] J. M. Hedgepeth. Pactruss support structure for precision segmented reflectors. NASA Contractor Report CR-181747, NASA, June 1989. AAC-TN-1153, ASTRO Aerospace Corporation, Carpinteria, CA.

[25] J. M. Hedgepeth. Structures for remotely deployable precision antennas. NASA Contractor Report CR-182065, NASA Langley Research Center, January 1989. Contract NAS1-12567. AAC-TN-1154, ASTRO Aerospace Corporation, Carpinteria, CA.

[26] I. W. Jones, C. Boateng, and C. D. Williams. An evaluation of foldable tubes for application in space structures. In *Proceedings of the 1985 SEM Spring Conference on Experimental Mechanics*, pages 590–598, Las Vegas, Nevada, June 9–14 1985. Society for Experimental Mechanics, Inc.

[27] H. Kellermeier, H. Vorbrugg, and K. Pontoppidan. The MBB unfurlable mesh antenna (UMA): design and development. In *Communications Satellite Systems Conference, Proceedings*, pages 417–425. AIAA, 1986.

[28] E. Lowe, M. Josephs, and J. Hedgepeth. Advanced deployable reflectors for communication satellites. In *AIAA/AHS/ASEE Aerospace Design Conference*, Irvine, CA, February 16–19 1993. AIAA 93-0978.

[29] P. K. Manhart and J. M. Rodgers. Segmented mirror manufacturing and alignment tolerances (smmat). JPL Publication 89-3, NASA Jet Propulsion Laboratory, California Institute of Technology, Pasadena, CA, March 1 1989.

[30] M. M. Mikulas, T. J. Collins, and J. M. Hedgepeth. Preliminary design considerations for 10-40 meter-diameter precision truss reflectors. *Journal of Spacecraft*, 28(4):439–447, July–August 1991.

[31] M. M. Mikulas and P. R. Withnell. Construction concepts for precision segmented reflectors. In *The 34th AIAA/ASME/ASCE/AHS/-ASC Structures, Structural Dynamics, and Materials Conference*, Part 3, pages 1360–1366, La Jolla, CA, April 19–22 1993. AIAA. AIAA-93-1461-CP.

[32] K. Miura and Y. Miyazaki. Concept of the tension truss antenna. *AIAA Journal*, 28(6):1098–1104, June 1990.

[33] K. Miura, T. Takano, T. Inoue, and K. Tanizawa. Structural design of a 10 m diameter tension truss antenna. In *42nd Congress of the International Astronautical Federation*, Montreal, Canada, October 5–11 1991.

IAF, 3-5, Rue Mario-Nikis, 75015 Paris, France. IAF-91-316.

[34] M. Natori, H. Furuya, S. Kato, Y. Takesita, and T. Sakai. A reflector concept using inflatable elements. In *Proceedings of the Sixteenth International Symposium on Space Technology and Science*, pages 459–467, Sapporo, 1988.

[35] M. C. Natori, K. Higuchi, K. Sekine, and K. Okazaki. Advanced concepts of inflatable rigidized structures for space applications. In *The 35th AIAA/ASME/ASCE/AHS/ASC Structures, Structural Dynamics, and Materials Conference*, Hilton Head, SC, April 18–20 1994. AIAA. AIAA 94-1473.

[36] M. C. Natori, T. Takano, T. Inoue, and T. Noda. Design and development of a deployable mesh antenna for MUSES-B spacecraft. In *The 34th AIAA/ASME/ASCE/AHS/ASC Structures, Structural Dynamics, and Materials Conference*, La Jolla, CA, April 19–22 1993. AIAA. AIAA 93-1460.

[37] G. Reibaldi, J. Hammer, M. C. Bernasconi, and E. Pagana. Inflatable space rigidized reflector development for land mobile missions. In *Communications Satellite Systems Conference, Proceedings*, pages 533–538. AIAA, 1986.

[38] A. G. Roederer and Y. Rahmat-Sahmii. Unfurlable satellite antennas: a review. *Annales des Telecommunications*, 44(9–10):475–488, 1989.

[39] C. A. Rogers, W. L. Stutzman, T. G. Campbell, and J. M. Hedgepeth. Technology assessment and development of large deployable antennas. *Journal of Aerospace Engineering*, 6(1):34–54, January 1993.

[40] J. E. Stumm and S. Kulick. Unfurlable, continuous-surface reflector concept. In R. L. Wright and T. G. Campbell, editors, *Earth Science Geostationary Platform Technology*, pages 129–136, Hampton, VA, 1989. Proceedings of workshop, September 21–22, 1988. NASA Conference Publication CP-3040.

[41] K. A. Takamatsu and J. Onoda. New deployable truss concepts for large antenna structures or solar concentrators. *Journal of Spacecraft*, 28(3):330–338, May–June 1991.

[42] Thompson Ramo Wooldridge, Inc. Sunflower solar collector. NASA Contractor Report CR-46, NASA, Washington, DC, May 1964. Contract NAS5-462.

[43] Z. You and S. Pellegrino. Deployable mesh reflector. In J. F. Abel, J. W. Leonard, and C. U. Penalba, editors, *Spatial, Lattice, and Tension Structures*, pages 103–112, Atlanta, Georgia, U.S.A., April 24–28 1994. International Association for Shell and Spatial Structures and Committee on Special Structures, Structural Division, ASCE, New York. Proceedings of the IASS–ASCE International Symposium held in conjunction with the ASCE Structures Congress XII.

[44] Z. You and S. Pellegrino. Dynamic deployment of the crts reflector. In *The 35th AIAA/ASME/ASCE/AHS/ASC Structures, Structural Dynamics, and Materials Conference*, Part 3, pages 1497–1505, Hilton Head, SC, April 18–20 1994. AIAA.

[45] Z. You and S. Pellegrino. Study of the folding and deployment aspects of a collapsible rib tensioned surface (CRTS) antenna reflector. European Space Agency Contract Report CUED/D-STRUCT/TR 144, University of Cambridge, Department of Engineering, Cambridge, CB2 1PZ, UK, March 15 1994.

Author biography

Gyula Greschik, a civil engineering graduate of the Technical University of Budapest, has received his PhD. in structural engineering from Cornell University in 1992 for his research on the computational mechanics of plastic stability phenomena in steel structures. His subsequent work at the University of Colorado has turned from an initial focus of software engineering and multi-body dynamics towards deployable structures in 1993. His contributions to the field are marked by inventions and papers on deployable mechanisms, inflatable structures, and antenna dish deployment.